1

Characteristics and source apportionment of fine haze aerosol in Beijing during the winter of 2013

4

5

6

Xiaona Shang[1], Kai Zhang[2*], Fan Meng[2], Shihao Wang[2], Meehye Lee[1*], Inseon Suh[1], Daegon Kim[3], Kwonho Jeon[3], Xuezhong Wang[2], Yuxi Zhao[2]

9

[1] Department of Earth & Environmental Sciences, Korea University, Seoul, South Korea

[2] State Key Laboratory of Environmental Criteria and Risk Assessment, Chinese Research Academy of Environmental Sciences, Beijing 100012, China

[3] Department of Climate & Air Quality Research, National Institution of Environmental Research, Incheon, South Korea

15

16

[*]Correspondence to: K. Zhang (zhangkai@craes.org.cn) or Meehye Lee (meehye@korea.ac.kr)

18

19

20

21

22

25

Abstract

For $PM_{2.5}$ filter samples collected daily at the Chinese Research Academy of Environmental Sciences (Beijing, China) from December of 2013 to February of 2014 (the winter period), chemical characteristics and sources were investigated with an emphasis on haze events in different alert levels. During the three months, the average $PM_{2.5}$ concentration was 89 µg m^{-3}, exceeding the Chinese national standard of 75 µg m^{-3} in 24 h. The maximum $PM_{2.5}$ concentration was 307 µg m^{-3}, which characterizes *developed-type* pollution ($PM_{2.5}/PM_{10} >$ 0.5) in the World Health Organization criteria. $PM_{2.5}$ was dominated by SO_4^{2-}, NO_3^-, and pseudo-carbonaceous compounds with obvious differences in concentrations and proportions between non-haze and haze episodes. The non-negative matrix factorization (NMF) analysis provided reasonable $PM_{2.5}$ source profiles, by which five sources were identified: soil dust, traffic emission, biomass combustion, industrial emission, and coal combustion accounting for 13 %, 22 %, 12 %, 28 %, and 25 %, respectively. The dust impact increased with northwesterlies during non-haze periods and decreased under stagnant condition during haze periods. A blue alert of heavy air pollution was characterized by the greatest contribution from industrial emissions (61 %). During the Chinese Lantern Festival, an orange-alert was issued and biomass combustion was found to be the major source owing to firecracker explosions. Red-alert haze was almost equally contributed by local traffic and transported coal combustion emissions from Beijing vicinities (approximately 40 % each) that was distinguished by the highest levels of NO_3^- and SO_4^{2-}, respectively. This study also reveals that the severity and source of haze are largely dependent on meteorological conditions.

Key words: $PM_{2.5}$, winter haze, Beijing, chemical composition, source apportionment, NMF

1. Introduction

With the increasing $PM_{2.5}$ concentration in northern China, winter haze occurrences increased from 3 to 16 days per year during 2000–2012 (Wang and Chen, 2016). The frequency of haze events during winter is enhanced by meteorological conditions; the minimum daily temperatures typically reach –15 to –20 °C (Wu et al., 2012) and the boundary layer height becomes shallow to less than 100 m (Zheng et al., 2015). Moreover, the combustion of fossil fuel increases at low temperatures (Zhang and Samet, 2015). As the air quality deteriorated, China released its third revision of the "The National Ambient Air Quality Standards" (NAAQS) in 2012 (GB 3095-2012), which stipulated safe $PM_{2.5}$ levels for the first time (Zhang and Cao, 2015). However, the worst haze events in the major cities of China were recorded during the winter of 2012–2013. During January of this period, Beijing experienced almost daily haze and the hourly $PM_{2.5}$ concentration reached 855 $\mu g\ m^{-3}$ (Zheng et al., 2015). In Beijing, winter haze episodes were 5 days in duration (Zheng et al., 2015, 2016). The long duration of haze with high $PM_{2.5}$ concentration triggers a red alert for air pollution (Liu et al., 2017), which is the highest level of the heavy air pollution warning system issued in the "Emergency plan for heavy air pollution in Beijing (revised in 2016)" (in Chinese: http://zhengce. beijing.gov.cn/ library/192/33/50/200/806828/96701/index.html).

The concentrations of SO_2, NO_x, and volatile organic compounds (VOCs), which are important precursors of $PM_{2.5}$, vary in different emission and policy implementations. Related particulate compositions (sulfate, nitrate, and organic matter) comprise two thirds of $PM_{2.5}$ (Huang et al., 2014; Hu et al., 2015). Over a seven-year period (2000–2006), SO_2 emission has increased by 53 %, consistent with the increases in power plant emissions from 10.6 Tg to 18.6 Tg (Lu et al., 2010). Particularly in northern China, the emissions from power plants have increased by 85 % over this period. In contrast, SO_2 levels have significantly decreased since 2006, when stricter SO_2 regulations, such as the use of flue-gas desulfurization systems or scrubbers, were imposed (Van der A et al., 2016). The reduction was particularly rapid during 2008–2009. On the other hand, the NO_x concentration increased from 2000 to 2012 (Hong et al., 2016; Cao et al., 2011). This increase is in accord with the increased number of vehicles, which contribute 90 % of the total NO_x emissions in Beijing (Hendrick et al., 2014;

81 Wu et al., 2012). Meanwhile, the continuous increase in VOC emissions (from 13 Tg/yr in
82 2000 to 26 Tg/yr in 2012) was mainly driven by industrial processes (~70 %) (Hong et al.,
83 2016). Coal combustion (especially that of raw coal) from households is underestimated in the
84 southern and eastern rural areas of Beijing. Rural coal combustion comprises approximately
85 75 % of Beijing's total coal combustion (Cheng et al., 2017). After the 2008 Olympic Games,
86 residential coal combustion emitted large amounts of SO_2, NO_x, and VOCs (70, 17, and 43 kt,
87 respectively). In 2013, these amounts had increased twofold to 132, 33, and 81 kt,
88 respectively. At the end of 2013, China issued the Air Pollution Prevention and Control
89 Action Plan (CAAC, 2013), which greatly reduced the precursor emissions in 2014 (Wang et
90 al., 2015).

91

92 Under the strict regulations on boiler and industrial emissions, SO_2 concentrations in Beijing
93 significantly decreased during the winter of 2013 and the fuel sulfur was reduced by more
94 than 80 % in 2014 (relative to its 2013 levels) (CAAC, 2013; CAAC, 2015). Over the same
95 period, the NO_x levels were reduced by 6.7 % over the nation, but exceeded the standard by
96 42 % in Beijing, where local traffic emissions remained high. Meanwhile, the $PM_{2.5}$ pollution
97 is the most severe in the region of southern Beijing, where the annual average concentration
98 reached 150 μg m^{-3} during 2014–2015. The level is comparable to the national standard of
99 PM_{10} (CAAC, 2015; Zhang and Cao, 2015).

100

101 Since the 2008 Olympics and 2013 CAACs, heavy industries have been relocated and high-
102 quality fuel has been introduced. Both actions have reduced the concentrations of gaseous
103 precursors (Wang et al., 2009; Van der A et al., 2016), although these reductions are in
104 contrast to the frequent hazes currently observed in Beijing. In recent studies, the $PM_{2.5}$, dust,
105 and SO_2 concentrations in Beijing have been mainly attributed to regional transport (Wang et
106 al., 2014; Yang et al., 2013; Wang et al., 2011). Considering the extreme haze situation in
107 Beijing, researchers have sought the crucial factors of haze formation, usually by identifying
108 the emission sources of $PM_{2.5}$. The source apportionment of $PM_{2.5}$ is commonly analyzed by
109 source receptor models such as positive matrix factorization (PMF) and non-negative matrix
110 factorization (NMF) (Reff et al., 2007; Kfoury et al., 2016). These models have implicated
111 coal and industries as major sources of $PM_{2.5}$ in Beijing (Huang et al., 2014; Zhang and Cao,

4

112   2015; Zhang et al., 2013).

113

114   Following the severe and frequent haze occurrences in January of 2013, the chemical

115   characteristics and sources of $PM_{2.5}$ in Beijing were extensively investigated (Jiang et al.,

116   2015; Zheng et al., 2015; Zhang et al., 2015; Chen et al., 2017). However, few studies have

117   investigated the winter season of 2013–2014, which immediately followed the enactment of

118   the 2013 CAAC in China. In particular, the source apportionment of Beijing's haze remains

119   unknown (Wu et al., 2016). In the present study, we thoroughly examine the chemical

120   compositions of $PM_{2.5}$ in Beijing during the winter of 2013–2014, and accordingly, diagnose

121   the haze occurrence, probe the local and transported influence on haze, and quantify the

122   critical source contributions.

123

124   **2. Experiments**

125

126   Filtered samples of PM_{10} and $PM_{2.5}$ were collected on the roof of a three-story container (~15

127   m above ground level) at the Chinese Research Academy of Environmental Sciences (CRAES)

128   in Beijing, China (40.04 °N, 116.42 °E), from December of 2013 to February of 2014. The

129   site is located near the four-way intersection of a residential area located between the 5th and

130   6th ring roads of Beijing.

131

132   Aerosols were collected for 24 hours (from 7 pm to 7 pm next day) on a 90-mm

133   polypropylene filter using a medium volume sampler at a flow rate of ~100 L/min (2030,

134   Laoying, China). Seventy $PM_{2.5}$ samples were collected and analyzed. The water-soluble ions

135   (Cl^-, NO_2^-, CO_3^{2-}, SO_4^{2-}, NO_3^-, Na^+, NH_4^+, K^+, Mg^{2+}, and Ca^{2+}) were measured by ion

136   chromatography (IC25, Dionex, USA) with a detection limit between 0.01 and 0.06 μg m^{-3}.

137   The ionic measurement method is detailed in Lim (2009). For trace elemental analysis, the

138   samples were digested by a mixture of acids as described in Zhang et al. (2014). A quarter of

139   each filter was placed into a polytetrafluoroethylene flask and digested with 8 mL of

140   HNO_3/H_2O_2 (6/2 v/v, superpure grade, Merck, Darmstadt) at 180 °C for 8 h. The solution was

141   separated by centrifugation and diluted to 25 mL with ultrapure water. The concentrations of

142 trace metals (21 species, including Si) were determined by inductively coupled plasma-optical

143 emission spectrometry (Prodigy 7, Teledyne Leeman, USA). The mass concentration of PM_{10}

144 was also determined for comparison with that of $PM_{2.5}$.

145

146 The total concentrations of the water-soluble ions and trace elements were subtracted from the

147 $PM_{2.5}$ mass, to provide a measure that likely represents the carbonaceous components that

148 were not directly measured. In this study, therefore, it was referred as the pseudo-

149 carbonaceous components and used for the following discussion. The concentrations of these

150 pseudo-carbonaceous components were comparable to those of $PM_{2.5}$ concentrations observed

151 in Beijing (Ji et al., 2016). A meteorological suite of relative humidity, temperature, and

152 visibility was collected by CRAES from a sharing network of the China Meteorological Data

153 Service Center (CMDC): http://data.cma.cn/en/?r=data/detail&dataCode=A.0012.0001. The

154 gaseous species NO_x, SO_2, CO, and O_3 were measured using commercial analyzers (42i, 43i,

155 48i, 49i, Thermo Fisher, USA) in CRAES.

156

157 The $PM_{2.5}$ source was identified by non-negative matrix factorization (NMF) analysis.

158 Introduced by Lee and Seung (1999, 2001), NMF operates similarly to positive matrix

159 factorization (PMF). Both analysis methods find two matrices (W and H, termed the

160 contribution matrix and the source profile matrix, respectively) that best reproduce the input

161 data matrix (V) using the same factorization approach (V = WH) as a positive constraint.

162 However, while PMF is a generalized, alternative least-squares method, NMF minimizes the

163 conventional least-squares error and the generalized Kullback–Leibler divergence. The

164 uncertainties in NMF analysis were estimated as 0.3 + the analytical detection limit (Xie et al.,

165 1999a, b).

166

167 In addition to NMF analysis, the origin of air masses was traced by trajectory analysis. For air

168 masses arriving at 500 m altitude, backward trajectories were computed for 72 hours using

169 HYSPLIT model with GDAS data in SplitR (Stein et al., 2015, https://github.com/rich-

170 iannone/ SplitR).

171

3. Characteristics of winter PM$_{2.5}$

3.1. PM$_{2.5}$ and PM$_{10}$ mass variations

During the 2013–2014 winter period in Beijing, the mass concentrations of PM$_{2.5}$ and PM$_{10}$ varied in a similar pattern (Fig. 1). Zheng et al. (2015) reported a similar trend between the PM$_{2.5}$ and PM$_{10}$ concentrations. In this study, the average PM$_{10}$ concentration was 142 µg m^{-3}, comparable to the Chinese national standard of 150 µg m^{-3} in 24 h (GB 3095-2012). However, the mean PM$_{2.5}$ concentration was 89 µg m^{-3}, exceeding the standard of 75 µg m^{-3} in 24 h. The PM$_{2.5}$ standard was most severely exceeded in February 2014, when the average concentration (133.5 µg m^{-3}) reached the highest winter concentration in Beijing during the 2005–2015 decade (Lang et al., 2017).

Based on the criteria of the World Health Organization (WHO) (2006), the wintertime air pollution of Beijing was classified as *developed-type*, meaning that the PM$_{2.5}$/PM$_{10}$ ratio exceeded 0.5 in 70 % of the samples (Table 1). The mean PM$_{2.5}$ concentration of these samples (113 µg m^{-3}) was four times higher than that in *developing-type* pollution (31 µg m^{-3}). In approximately half of the *developed-type* samples, the PM$_{2.5}$ and PM$_{10}$ mass concentrations exceeded the national standards, all of which were collected during haze events. The average PM$_{2.5}$ concentration over 13 haze days reached 198 µg m^{-3} and the visibility was significantly reduced to ~1 km (Fig. 1). In contrast, the PM$_{2.5}$ concentration exceeded the standard without violating the PM$_{10}$ concentration on only a few days. These results well reflect the wintertime characteristics of PM$_{2.5}$ levels in Beijing, which are largely related to haze episodes. The average PM$_{2.5}$ concentration of the *developed-type* was comparable to that of the *developing-type* unless the PM$_{2.5}$ concentration exceeded the standard.

On 12 out of 13 haze days, the pollutant levels met the criteria of heavy air pollution alerts stipulated in the "Emergency plan for heavy air pollution in Beijing (revised in 2016)". In the lowest level of the four-tier warning system, blue alert, the daily average air quality index (AQI) exceeded 200 on only one day. In Table 1, the one no-alert and three blue-alert haze days are defined as no/blue-alert haze events. The average PM$_{2.5}$ concentration on these days was 168 µg m^{-3} (Table 1). During the red-alert period (February 20–25), the daily PM$_{2.5}$

203 concentration peaked at 306 µg m^{-3}. A red alert is declared when the air pollution is heavy and
204 severe. During a red alert, AQI exceeds 200 on four consecutive days and exceeds 300 on
205 continuous two of those days. Although the daily average AQI remained higher than 300
206 during the February 14–16 period, this event was an orange alert because it continued for only
207 three days. The AQI data can be found at http://www.tianqihoubao.com/aqi/beijing-
208 201402.html (in Chinese). Here, we describe episodes in terms of alerts defined in the heavy
209 air pollution system rather than in the haze alert system, because the former definition is
210 based on the daily averaged AQI, whereas the three-tier haze warnings depend on the hourly
211 meteorological parameters (relative humidity and visibility) or PM$_{2.5}$. Because we measured
212 the daily concentrations, the heavy air pollution alert was suitable for our purpose.

3.2. Chemical composition

214

215 Throughout the wintertime, the average PM$_{2.5}$ concentration remained close to 90 µg m^{-3}, 20 %
216 above the national standard. The major PM$_{2.5}$ components were SO_4^{2-}, NO_3^-, NH_4^+, and
217 pseudo-carbonaceous compounds, with average concentrations of 18.8, 16.9, 8.5, and 38.6 µg
218 m^{-3}, respectively. Collectively, these four compositions comprised 83 % of the PM$_{2.5}$ mass
219 (Fig. 2). On the 57 non-haze days, the fractional chemical compositions and concentrations of
220 SO$_2$ and NO$_2$ were comparable to those of the entire period (70 days). In contrast, the portions
221 of soil minerals such as Ca^{2+} and trace elements (including Si) were 3–4 times higher on non-
222 haze days than on haze days. The Ca^{2+} and Si concentrations were highly correlated ($r^2 = 0.8$)
223 and were more related to the PM$_{10}$ ($r^2 = 0.6$) than PM$_{2.5}$ levels. This reflects the significant
224 impact of soil dust on non-haze days (Fu et al., 2012). On haze days, the particle masses,
225 compositions, SO$_2$, and NO$_2$ varied widely among the different alert levels.

226

3.3. Source profiles

228

229 The PM$_{2.5}$ sources were identified in an NMF analysis of the measurement data. The data
230 included 8 water-soluble ions, 13 trace elements, and pseudo-carbonaceous compounds. After
231 comparison through a principle component analysis, the principal factors were determined.

8

Finally, five critical factors were distinguished: soil dust, traffic emission, biomass combustion, industrial emission, and coal combustion (Table 2). The five source profiles are presented in Figure 3. Despite their clear signatures, the contributions of dust and traffic emissions were approximately half those of biomass combustion, industrial emission, and coal combustion (Table 2).

Factor 1 (soil dust) is confirmed by high Ca^{2+}, Si, Fe, Cl^-, and Na^+ contents (Fu et al., 2012). The high concentrations of Cl^- and Na^+ likely originate from dry lake deposits (Abuduwaili et al., 2015), which spread over the northern area of Beijing. Elevated heavy metals suggest the presence of fugitive dust mixed with industry or traffic emissions (Wan et al., 2016). The high loadings of NO_3^- and NH_4^+ in Factor 2 indicate traffic emissions (He et al., 2016). As is well known, NH_3 is emitted from three-way catalytic converters in vehicles (Chang et al., 2016). Factor 3 (biomass combustion) emits large amounts of K^+ and NH_4^+ (Balasubramanian et al., 1999), along with the elements that give exploding fireworks their color (namely Mg, Fe, Al, Ti, Cu, and Si) (Baranyai et al., 2015). The concentrations of these firecracker indicators are most significantly elevated during the Chinese Lantern Festival (14, 15, and 16 of February; Fig. 1). Factor 4 (industrial emissions) is distinguished by high pseudo-carbonaceous materials and heavy metals. Factor 5 (coal combustion) is characterized by high Cl^-, SO_4^{2-}, and NO_3^- contributions, which are absent in Factor 4. Although both Factors 4 and 5 represent the influence of industrial emissions near Beijing, Factor 5 is more clearly sourced from industries requiring high energy, such as iron and steel, cement, and power plants (Tan et al., 2016; Zhang et al., 2013). In contrast, Factor 4 indicates emissions from industrial processes using VOCs as raw materials such as furniture manufacturing, petroleum refining, machinery equipment manufacturing and printing (Wu et al., 2015).

In a previous study, source apportionment by NMF or PMF analysis distinguished 7–8 factors (Zhang et al., 2013), including a secondary formation source. The secondary source was not separated as an individual factor in the present study. As a typical secondary species, SO_4^{2-} dominates in Factor 5. However, a NO_3^- signature appears in all factors except Factor 4. As a megacity, Beijing is surrounded by large satellite cities with industrial complexes. Thus, Beijing is susceptable to emissions from these areas in addition to its own emissions, when

meteorological conditions are met. This will be discussed in detail in the following section. In fact, the atmospheric condition facilitated haze occurrence, leading to the major sources and the degree of aging for aerosols being intimately coupled. Therefore, these five factors primarily represent direct emission sources with secondary sources being implicitly included. In addition, NO_2 is more likely sourced from local emissions, but SO_2 is expected to be transported from nearby regions.

4. Characteristics of winter haze

4.1. Chemical and meteorological characteristics

The chemical compositions of $PM_{2.5}$ clearly differed on haze in contrast to non-haze days in terms of secondary ions and pseudo-carbonaceous compounds (Fig. 2). The largest fraction of pseudo-carbonaceous compounds (61 %) was accompanied with the smallest proportion of SO_4^{2-} (4%) on no/blue-alert days, suggesting low coal consumption by high-VOC-emitting industries. On orange-alert haze events, the NO_3^- fraction was twice that on non-haze days, and the K^+ and Mg^{2+} proportions were maximized (at 6 % and 1 %, respectively), implying biomass-combustion emission during the Lantern festival in China. The concentrations of SO_4^{2-} and NO_3^- were comparable with the greatest contribution in red-alert haze events. In addition, these species were closely related to the Cl^- ($r^2 = 0.8$) and NH_4^+ ($r^2 = 0.9$) concentrations, respectively, suggesting large contributions by coal combustion and vehicle emission. It is also noteworthy that the SO_4^{2-} fraction varied more widely than the NO_3^- fraction (Table S1). Among the three levels of haze events, SO_4^{2-} varied from 4 % to 32 %, whereas NO_3^- varied from 16 % to 31 % and NH_4^+ from 9 % to 11 %. Similarly, although both SO_2 and NO_2 concentrations were the highest in red-alert haze, SO_2 enhancement (relative to non-haze days) was 20 % larger than NO_2 enhancement. Because the sulfur compounds were much more elevated than the nitrogen compounds on haze days (particularly in red-alert haze events), the winter haze in Beijing was concluded to be largely contributed by coal combustion, which emits sulfur compounds. Furthermore, coal emissions are mostly transported from nearby Beijing (Hendrick et al., 2014).

To examine the meteorological conditions favorable for haze occurrence and clarify the

emission source regions, surface weather maps combined with daily average backward trajectories at 500 m were compared during non-haze and haze events. Previous studies also reported that weather conditions were critical for haze formation. In East China, migratory anticyclones and weak pressure gradients were the prerequisites of winter haze from 1980 to 2012 (Peng et al., 2016). High $PM_{2.5}$ episodes in Beijing usually began with weak southerly winds and ended with strong northerly winds (Guo et al., 2014). In this study, the air mass was usually transported from the northwest. As the high pressure system expanded, however, it was trasnported from the west, southwest, and southeast. Throughout this process, the weather condition became increasingly stagnant (Fig. 4) and the haze-alert level increased gradually. The recent study also emphasized the effect of meteorological condition on the severity of haze in Beijing (Cai et al., 2017). When air masses were rapidly transported from the northern desert area (Fig. 4a), mineral species such as Ca^{2+} and Si were enriched on non-haze days and the PM_{10} mass was high. In the western regions of Beijing (Fig. 4b), where various industries manufacture food, drink, furniture, pharmaceuticals, and other products from VOCs (http://www.berkeleysg.com/2016/06/china-manufacturing-distribution-map/), the fraction of pseudo-carbonaceous compounds rose to its maximum as the air mass slightly lingered over the region. During February 14–16, firecracker explosions caused a spike in K^+, Mg^{2+}, and NH_4^+ concentration under the stagnant weather condition, in which the air mass moved very slowly from the southwestern areas, where population density is the highest (Cheng et al., 2017). As the air mass moved eastward toward the high energy-requiring regions (http://berc.berkeley.edu/energy-access-developing-parts-china/) (Fig. 4d), such as Tianjin and Tangshan, where coal consumption is high for industrial use and residential heating (Cheng et al., 2017), the $PM_{2.5}$ and SO_4^{2-} (SO_2) concentrations reached their maxima.

4.2. Source profiles

To quantify each source contribution during the winter haze in Beijing, daily samples were analyzed by NMF and the source profiles during haze and non-haze episodes were compared (Fig. 5). In all samples, the main contributions were industrial, traffic, and coal combustion emissions (22–28 %), followed by soil dust and biomass combustion (13 % and 12 %, respectively). However, soil dust loading, which is associated with elevated fractions of Ca,

Si, and pseudo-carbonaceous matters (Fig. 2), was enhanced to 20 % during non-haze events. Meanwhile, the local traffic contribution decreased as the air mass was rapidly transported from the northwestern desert areas, as mentioned in subsection 4.1.

The three types of haze episodes exhibited strong contrasts not only in their chemical species and source regions, as mentioned above, but also in their source profiles (Fig. 5). No/blue-alert haze was dominated by industrial emissions (61 %) as the airflow passed over the industrial regions manufacturing products from raw VOCs. Consequently, the pseudo-carbonaceous concentration increased. During orange- and red-alert haze events, the dust contribution was negligible and the anthropogenic fraction increased sharply. During the Chinese Lantern Festival (which triggered an orange alert), a biomass signature with the highest K^+ concentration was observed in the air mass transported from the southwestern populated areas of Beijing. The K^+ contribution (35 %) was three times higher than that on non-haze days. During February 20–25, the outflow of the high coal-consuming eastern region enhanced the proportion of coal combustion products to 37 %. Simultaneously, the traffic contribution was the highest at 43 %. The coal and traffic effects were accompanied by two-fold elevations of SO_4^{2-} and NO_3^- in $PM_{2.5}$.

5. Policy implications

During the 2013–2014 winter period in Beijing, the average $PM_{2.5}$ concentration exceeded the standard by 20 %, and in February, reached its highest level in the 2005–2015 decade (Lang et al., 2017). The $PM_{2.5}$ mass closure and concentration of gaseous precursors during the 57 non-haze days were comparable to those of the entire winter period. Mineral dust is an important source of $PM_{2.5}$ and elevates the PM_{10} concentration on non-haze days. The average $PM_{2.5}$ concentrations increased significantly from 65 µg m^{-3} on non-haze days to 168 µg m^{-3} on no/blue-alert days and to 218 µg m^{-3} on red-alert days.

When weather conditions stagnate under weak pressure gradients, the alert levels of heavy air pollution upgrade on haze days. The migratory anticyclones also shift the air masses, causing

wide variations in chemical species and emission sources. During haze days, the NO_2 and NO_3^- concentrations exceed those of SO_2 and SO_4^{2-}, respectively, but the sulfur-containing species vary more widely than the nitrogen species. The sulfur compounds are particularly enhanced in stagnant air masses transported from the Beijing vicinities, including the southern and eastern regions, leading to the large sulfur variation with little change in nitrogen. These results highlights the significant influence of the emissions from industries requiring high energy and using coal in Beijing vicinities and from local vehicles on winter haze formation in Beijing, which is in accordance with findings from previous studies (Hendrick et al., 2014; Wang et al., 2016). To abate the severe haze in Beijing, therefore, it is necessary to reduce vehicle emissions in Beijing and further sulfur emissions from industrial complexes and uncontrolled coal combustion in surrounding cities. For cost-effectiveness, the weather forecast needs to be incorporated into the policy implementation.

6. Conclusion

This study investigated the chemical characteristics of $PM_{2.5}$ during the 2013–2014 winter period in Beijing and identified its sources with an emphasis on haze events by measuring the particle masses, water-soluble ions, and trace elements in filtered samples. Finally, policy implications for controlling haze occurrences in Beijing were deduced from the analysis.

The samples were collected daily at CRAES, Beijing, China, from December of 2013 to February of 2014. During the winter period, the overall average $PM_{2.5}$ concentration in Beijing was 89 μg/m^3, exceeding the Chinese national standard of 75 μg/m^3 in 24 h. The excess was linked to high occurrence of haze events in February of 2014. The high $PM_{2.5}$ episodes were concurrent with PM_{10} exceedance. Seventy percent of the samples were identified as *developed-type* in the WHO criteria; that is, their $PM_{2.5}/PM_{10}$ ratios exceeded 0.5. All 13 recognized haze events in this study were included in the *developed-type*.

The chemical compositions showed that secondary ions were doubled on haze days relative to non-haze days, but mineral species were halved during haze events. For the 70 daily $PM_{2.5}$

13

385   samples, NMF analysis was performed and the source profiles were compared between haze

386   and non-haze days. The analysis identified five principle sources, of which industrial emission,

387   coal combustion, and traffic emission comprised similar fractions of 28 %, 25 %, and 22 %,

388   respectively. The soil-dust and biomass-combustion sources were well distinguished and

389   contributed 13 % and 12 %, respectively. Comparing the source profiles between non-haze

390   and haze events, the impact of soil dust was most noticeable on non-haze days, when the air

391   masses rapidly transported from northwestern desert areas and brought high concentrations of

392   Ca^{2+} and Si into Beijing. However, nearby transport of industrial, biomass combustion, and

393   coal combustion emissions, along with local traffic emission, contributed to haze events under

394   stagnant weather conditions. The contributions of these four sources increased by up to 61 %,

395   35 %, 37 %, and 43 % in no/blue-alert, orange-alert, and red-alert days, respectively. The

396   industries that are mainly located to the west of Beijing use VOCs as raw materials, elevating

397   the pseudo-carbonaceous components in $PM_{2.5}$. Biomass combustion increases during the

398   firework displays of the Lantern Festival (February 14–16). At that time, the K^+ and Mg^{2+}

399   concentrations are maximized. When a red-alert was issued for six days in 2014, the

400   contribution of SO_4^{2-} and NO_3^- increased by factors of 3 and 2, respectively, from their non-

401   haze levels. Overall, the sulfur compounds (SO_2 and SO_4^{2-}) varied much more widely than the

402   nitrogen compounds (NO_2 and NO_3^-) through haze events, implying the substantial

403   contribution of industrial emissions from coal combustion in surrounding cities. The high

404   level of nitrogen compounds suggests local vehicle emissions as a main source of winter haze

405   in Beijing. This study also emphasizes the role of weather condition in haze formation by

406   building up stagnant condition that facilitates the transport of industrial emissions from

407   Beijing vicinities. These findings will be applicable to policy making.

408

409

410   **Acknowledgements**

411

References

Abuduwaili, J., Zhaoyong, Z., Jiang, F., and Liu, D.: The disastrous effects of salt dust deposition on cotton leaf photosynthesis and the cell physiological properties in the Ebinur basin in northwest China, PloS one, 10, e0124546, doi.org/10.1371/journal.pone.0124546, 2015.

Balasubramanian, R., Victor, T., and Begum, R.: Impact of biomass burning on rainwater acidity and com-position in Singapore, J. Geophys. Res., 104, 26881-26890, doi: 10.1029/1999JD900247, 1999.

Baranyai, E., Simon, E., Braun, M., Tóthmérész, B., Posta, J., and Fábián, I.: The effect of a fireworks event on the amount and elemental concentration of deposited dust collected in the city of Debrecen, Hungary, Air Qual. Atmos. Health, 8, 359-365, doi:10.1007/s11869-014-0290-7, 2015.

CAAC 2013, Clean Air Alliance of China, State Council air pollution prevention and control action plan, issue II, October 2013, http://en.cleanairchina.org/product/6346.html (English translation). Last accessed: 8 October 2015.

CAAC 2015, Clean Air Alliance of China, China Air Quality Management Assessment Report, Issue II, December 2015, http://en.cleanairchina.org/product/7386.html (English translation).

Cai, W., Li, K., Liao, H., Wang, H., and Wu, L.: Weather conditions conducive to Beijing severe haze more frequent under climate change, Nat. Clim. Change, 7, 257–262, doi:10.1038/nclimate3249, 2017.

Cao, G. L., Zhang, X. Y., Gong, S. L., An, X. Q., and Wang, Y. Q.: Emission inventories of primary particles and pollutant gases for China, Chinese Sci. Bull., 56, 781–788, doi:10.1007/s11434-011-4373-7, 2011.

Chang, Y., Zou, Z., Deng, C., Huang, K., Collett, J. L., Lin, J., and Zhuang, G.: The importance of vehicle emissions as a source of atmospheric ammonia in the megacity of Shanghai, Atmos. Chem. Phys., 16, 3577–3594, doi:10.5194/acp-16-3577-2016, 2016.

Chen, F., Zhang, X., Zhu, X., Zhang, H., Gao, J., and Hopke, P. K.: Chemical characteristics of $PM_{2.5}$ during a 2016 winter haze episode in Shijiazhuang, China, Aerosol Air Qual. Res., 17, 368-380, doi: 10.4209/aaqr.2016.06.0274, 2017.

454 Cheng, M., Zhi, G., Tang, W., Liu, S., Dang, H., Guo, Z., and Meng, F.: Air pollutant
455   emission from the underestimated households' coal consumption source in China, Sci.
456   Total Environ., 580, 641-650, 2017.

457 Fu, Z., Zhai, Y., Wang, L., Zeng, G., Li, C., Peng, W., and Lu, P.: Morphological,
458   geochemical composition and origins of near-surface atmospheric dust in Changsha city of
459   China, Environ. Earth Sci., 66, 2207-2216, doi:10.1007/s12665-011-1442-9, 2012.

460 Guo, S., Hu, M., Zamora, M. L., Peng, J., Shang, D., Zheng, J., and Molina, M. J.:
461   Elucidating severe urban haze formation in China, Proc. Natl. Acad. Sci., 111, 17373-
462   17378, doi: 10.1073/pnas.1419604111, 2014.

463 He, J., Wu, L., Mao, H., Liu, H., Jing, B., Yu, Y., Ren, P., Feng, C., and Liu, X.:
464   Development of a vehicle emission inventory with high temporal–spatial resolution based
465   on NRT traffic data and its impact on air pollution in Beijing – Part 2: Impact of vehicle
466   emission on urban air quality, Atmos. Chem. Phys., 16, 3171-3184, doi:10.5194/acp-16-
467   3171-2016, 2016.

468 Hendrick, F., Müller, J.-F., Clémer, K., Wang, P., De Mazière, M., Fayt, C., Gielen, C.,
469   Hermans, C., Ma, J. Z., Pinardi, G., Stavrakou, T., Vlemmix, T., and Van Roozendael, M.:
470   Four years of ground-based MAX-DOAS observations of HONO and NO_2 in the Beijing
471   area, Atmos. Chem. Phys., 14, 765-781, doi:10.5194/acp-14-765-2014, 2014.

472 Hong, C., Zhang, Q., He, K., Guan, D., Li, M., Liu, F., and Zheng, B.: Variations of China's
473   emission estimates response to uncertainties in energy statistics, Atmos. Chem. Phys.
474   Discuss., doi:10.5194/acp-2016-459, in review, 2016.

475 Hu, G., Sun, J., Zhang, Y., Shen, X., and Yang, Y.: Chemical composition of $PM_{2.5}$ based on
476   two-year measurements at an urban site in Beijing, Aerosol Air Qual. Res., 15, 1748-1759,
477   doi: 10.4209/aaqr.2014.11.0284, 2015.

478 Huang, R. J., Zhang, Y., Bozzetti, C., Ho, K. F., Cao, J. J., Han, Y., and Zotter, P.: High
479   secondary aerosol contribution to particulate pollution during haze events in China, Nature,
480   514, 218-222, doi:10.1038/nature13774, 2014.

481 Ji, D., Zhang, J., He, J., Wang, X., Pang, B., Liu, Z., and Wang, Y.: Characteristics of
482   atmospheric organic and elemental carbon aerosols in urban Beijing, China, Atmos.
483   Environ., 125, 293-306, doi.org/10.1016/j.atmosenv.2015.11.020, 2016.

484 Jiang, J., Zhou, W., Cheng, Z., Wang, S., He, K., and Hao, J.: Particulate matter distributions
485   in China during a winter period with frequent pollution episodes (January 2013), Aerosol
486   Air Qual. Res., 15, 494-503, doi: 10.4209/aaqr.2014.04.0070, 2015.

487 Kfoury, A., Ledoux, F., Roche, C., Delmaire, G., Roussel, G., and Courcot, D.: $PM_{2.5}$ source
488   apportionment in a French urban coastal site under steelworks emission influences using
489   constrained non-negative matrix factorization receptor model, J. Environ. Sci., 40, 114-128,
490   doi.org/10.1016/j.jes.2015.10.025, 2016.

491 Lang, J., Zhang, Y., Cheng, S., Zhou, Y., Chen, D., Guo, X., Li, X., Xing, X., Chen, S., and
492   Wang, H.: Trends of $PM_{2.5}$ and chemical composition in Beijing, 2000-2015, Aerosol Air
493   Qual. Res., 17, 412–425, doi: 10.4209/aaqr.2017.01.0042, 2017.

494 Lee, D. D. and Seung, H. S.: Learning the parts of objects by non-negative matrix
495   factorization, Nature, 401, 788-791, doi:10.1038/44565, 1999.

496 Lee, D. D. and Seung, H. S.: Algorithms for non-negative matrix factorization, Adv. Neural.
497   Inf. Process Syst., 13, 556–562, 2001.

498 Liu, T., Gong, S., He, J., Yu, M., Wang, Q., Li, H., Liu, W., Zhang, J., Li, L., Wang, X., Li, S.,
499   Lu, Y., Du, H., Wang, Y., Zhou, C., Liu, H., and Zhao, Q.: Attributions of meteorological
500   and emission factors to the 2015 winter severe haze pollution episodes in China's Jing-Jin-
501   Ji area, Atmos. Chem. Phys., 17, 2971-2980, doi:10.5194/acp-17-2971-2017, 2017.

502 Lim, S.: Source Signature of Ions and Carbonaceous Compounds in Submicron and
503   Supermicron Aerosols at Gosan-super site, Jeju, South Korea, Master's thesis, Korea
504   University, 2009.

505 Lu, Z., Streets, D. G., Zhang, Q., Wang, S., Carmichael, G. R., Cheng, Y. F., Wei, C., Chin,
506   M., Diehl, T., and Tan, Q.: Sulfur dioxide emissions in China and sulfur trends in East
507   Asia since 2000, Atmos. Chem. Phys., 10, 6311-6331, doi:10.5194/acp-10-6311-2010,
508   2010.

509 Ministry of Environmental Protection of the People's Republic of China, Ambient air quality
510   standards (GB3095-2012), Chinese Environmental Science Press: Beijing, China, 2012 (in
511   Chinese).

512 Peng, H., Liu, D., Zhou, B., Su, Y., Wu, J., Shen, H., Wei, J., and Cao, L.: Boundary-layer
513   characteristics of persistent regional haze events and heavy haze days in eastern China,

514   Adv. Meteorol., 6950154, doi.org/10.1155/2016/6950154, 2016.

515   Reff, A., Eberly, S., and Bhave, P.: Receptor modeling of ambient particulate matter data
516   using positive matrix factorization: review of existing methods, J. Air Waste Manage.
517   Assoc., 2007.

518   Stein, A.F., Draxler, R.R, Rolph, G.D., Stunder, B.J.B., Cohen, M.D., and Ngan, F.: NOAA's
519   HYSPLIT atmospheric transport and dispersion modeling system, Bull. Amer. Meteor.
520   Soc., 96, 2059-2077, http://dx.doi.org/10.1175/BAMS-D-14-00110.1, 2015.

521   Tan, J., Duan, J., Zhen, N., He, K., and Hao, J.: Chemical characteristics and source of size-
522   fractionated atmospheric particle in haze episode in Beijing, Atmos. Res., 167, 24-33,
523   10.1016/j.atmosres.2015.06.015, 2016.

524   Van der A, R. J., Mijling, B., Ding, J., Koukouli, M. E., Liu, F., Li, Q., Mao, H., and Theys,
525   N.: Cleaning up the air: Effectiveness of air quality policy for SO_2 and NO_x emissions in
526   China, Atmos. Chem. Phys. Discuss., doi:10.5194/acp-2016-445, in review, 2016.

527   Wan, D., Han, Z., Yang, J., Yang, G., and Liu, X.: Heavy metal pollution in settled dust
528   associated with different urban functional areas in a heavily air-polluted city in North
529   China, Int. J. Environ. Res. Public Health, 13, E1119, doi: 10.3390/ijerph13111119, 2016.

530   Wang, H.-J. and Chen, H.-P.: Understanding the recent trend of haze pollution in eastern
531   China: roles of climate change, Atmos. Chem. Phys., 16, 4205-4211, doi:10.5194/acp-16-
532   4205-2016, 2016.

533   Wang, G., Zhang, R., Gomez, M. E., Yang, L., Zamora, M. L., Hu, M., and Li, J.: Persistent
534   sulfate formation from London Fog to Chinese haze, Proc. Natl. Acad. Sci., 113, 13630-
535   13635, doi: 10.1073/pnas.1616540113, 2016.

536   Wang, L. T., Wei, Z., Yang, J., Zhang, Y., Zhang, F. F., Su, J., Meng, C. C., and Zhang, Q.:
537   The 2013 severe haze over southern Hebei, China: model evaluation, source apportionment,
538   and policy implications, Atmos. Chem. Phys., 14, 3151-3173, doi:10.5194/acp-14-3151-
539   2014, 2014.

540   Wang, M., Zhu, T., Zhang, J. P., Zhang, Q. H., Lin, W. W., Li, Y., and Wang, Z. F.: Using a
541   mobile laboratory to characterize the distribution and transport of sulfur dioxide in and
542   around Beijing, Atmos. Chem. Phys., 11, 11631-11645, doi:10.5194/acp-11-11631-2011,
543   2011.

Wang, M., Zhu, T., Zheng, J., Zhang, R. Y., Zhang, S. Q., Xie, X. X., Han, Y. Q., and Li, Y.: Use of a mobile laboratory to evaluate changes in on-road air pollutants during the Beijing 2008 Summer Olympics, Atmos. Chem. Phys., 9, 8247-8263, doi:10.5194/acp-9-8247-2009, 2009.

Wang, Y., Yao, L., Wang, L., Liu, Z., Ji, D., Tang, G., Zhang, J., Sun, Y., Hu, B., and Xin, J.: Mechanism for the formation of the January 2013 heavy haze pollution episode over central and eastern China, Sci. China Earth Sci., 57, 14–25, 2014.

Wang, Y. Q., Zhang, X. Y., Sun, J. Y., Zhang, X. C., Che, H. Z., and Li, Y.: Spatial and temporal variations of the concentrations of PM_{10}, $PM_{2.5}$ and PM_1 in China, Atmos. Chem. Phys., 15, 13585-13598, doi:10.5194/acp-15-13585-2015, 2015.

World Health Organization: Air quality guidelines: global update 2005: particulate matter, ozone, nitrogen dioxide, and sulfur dioxide, World Health Organization, 2006.

Wu, J., Zhang, P., Yi, H., and Qin, Z.: What causes haze pollution? An empirical study of $PM_{2.5}$ concentrations in Chinese cities, Sustainability, 8, 132, doi:10.3390/su8020132, 2016.

Wu, S., Lu, A., and Li, L.: Spatial and temporal characteristics of minimum temperature in winter in China during 1961–2010 from NCEP/NCAR reanalysis, Theor. Appl. Climatol., 108, 207–216, doi: 10.1007/s00704-011-0525-6, 2012.

Wu, X., Huang, W., Zhang, Y., Zheng, C., Jiang, X., Gao, X., and Cen, K.: Characteristics and uncertainty of industrial VOCs emissions in China, Aerosol Air Qual. Res., 15, 1045-1058, doi: 10.4209/aaqr.2014.10.0236, 2015.

Xie, Y. L., Hopke, P. K., Paatero, P., Barrie, L. A., and Li, S. M.: Identification of Source Nature and Seasonal Variations of Arctic Aerosol by positive matrix factorization, J. Atmos. Sci., 56, 249–260, 1999a.

Xie, Y. L., Hopke, P. K., Paatero, P., Barrie, L. A., and Li, S. M.: Identification of source nature and seasonal variations of Arctic aerosol by the multilinear engine, Atmos. Environ., 33, 2549-2562, doi.org/10.1016/S1352-2310(98)00196-4, 1999b.

Yang, K., Dickerson, R. R., Carn, S. A., Ge, C., and Wang, J.: First observations of SO2 from the satellite Suomi NPP OMPS: Widespread air pollution events over China, Geophys. Res. Lett., 40, 4957–4962, 2013.

574 Zhang, J. J. and Samet, J. M.: Chinese haze versus Western smog: lessons learned, J. Thorac.

575 Dis., 7, 3, doi: 10.3978/j.issn.2072-1439.2014.12.06, 2015.

576 Zhang, K., Chai, F., Zheng, Z., Yang, Q., Li, J., Wang, J., and Zhang, Y.: Characteristics of

577 atmospheric particles and heavy metals in winter in Chang-Zhu-Tan city clusters, China, J.

578 Environ. Sci., 26, 147-53, 2014.

579 Zhang, Y. L. and Cao, F.: Fine particulate matter ($PM_{2.5}$) in China at a city level, Sci. Reports,

580 5. 14884, doi: 10.1038/srep14884, 2015.

581 Zhang, R., Jing, J., Tao, J., Hsu, S.-C., Wang, G., Cao, J., Lee, C. S. L., Zhu, L., Chen, Z.,

582 Zhao, Y., and Shen, Z.: Chemical characterization and source apportionment of $PM_{2.5}$ in

583 Beijing: seasonal perspective, Atmos. Chem. Phys., 13, 7053-7074, doi:10.5194/acp-13-

584 7053-2013, 2013.

585 Zheng, G. J., Duan, F. K., Su, H., Ma, Y. L., Cheng, Y., Zheng, B., Zhang, Q., Huang, T.,

586 Kimoto, T., Chang, D., Pöschl, U., Cheng, Y. F., and He, K. B.: Exploring the severe

587 winter haze in Beijing: the impact of synoptic weather, regional transport and

588 heterogeneous reactions, Atmos. Chem. Phys., 15, 2969-2983, doi:10.5194/acp-15-2969-

589 2015, 2015.

590 Zheng, G., Duan, F., Ma, Y., Zhang, Q., Huang, T., Kimoto, T., and He, K.: Episode-based

591 evolution pattern analysis of haze pollution: method development and results from Beijing,

592 China, Environ. Sci. Technol., 50, 4632-4641, doi: 10.1021/acs.est.5b05593, 2016.

593 **Table 1.** Statistics of $PM_{2.5}$ mass concentrations.

$PM_{2.5}$ mass classification	Number	$PM_{2.5}^{*}$ [$\mu g\ m^{-3}$]
Chemical and NMF analysis	70	
Comparison with PM_{10} mass	67	89
$PM_{2.5}/PM_{10} > 0.5$	47	113
$PM_{2.5} > 75\ \mu g\ m^{-3}$ and $PM_{10} > 150\ \mu g\ m^{-3}$	23	168
$PM_{2.5} > 75\ \mu g\ m^{-3}$ and $PM_{10} < 150\ \mu g\ m^{-3}$	5	113
$PM_{2.5} < 75\ \mu g\ m^{-3}$ and $PM_{10} < 150\ \mu g\ m^{-3}$	19	39
$PM_{2.5}/PM_{10} \leq 0.5$	20	31
Haze days[#]	13	198
Red alert	6	218
Orange alert	3	216
No/blue alert	4	168

594 * Average concentration

595 [#] Heavy air pollution alert

596 **Table 2.** Sources identified by NMF analysis.

| Factor	Contribution	Sources
Factor 1	13 %	Soil dust
Factor 2	22 %	Traffic emission
Factor 3	12 %	Biomass combustion
Factor 4	28 %	Industrial emission
Factor 5	25 %	Coal combustion
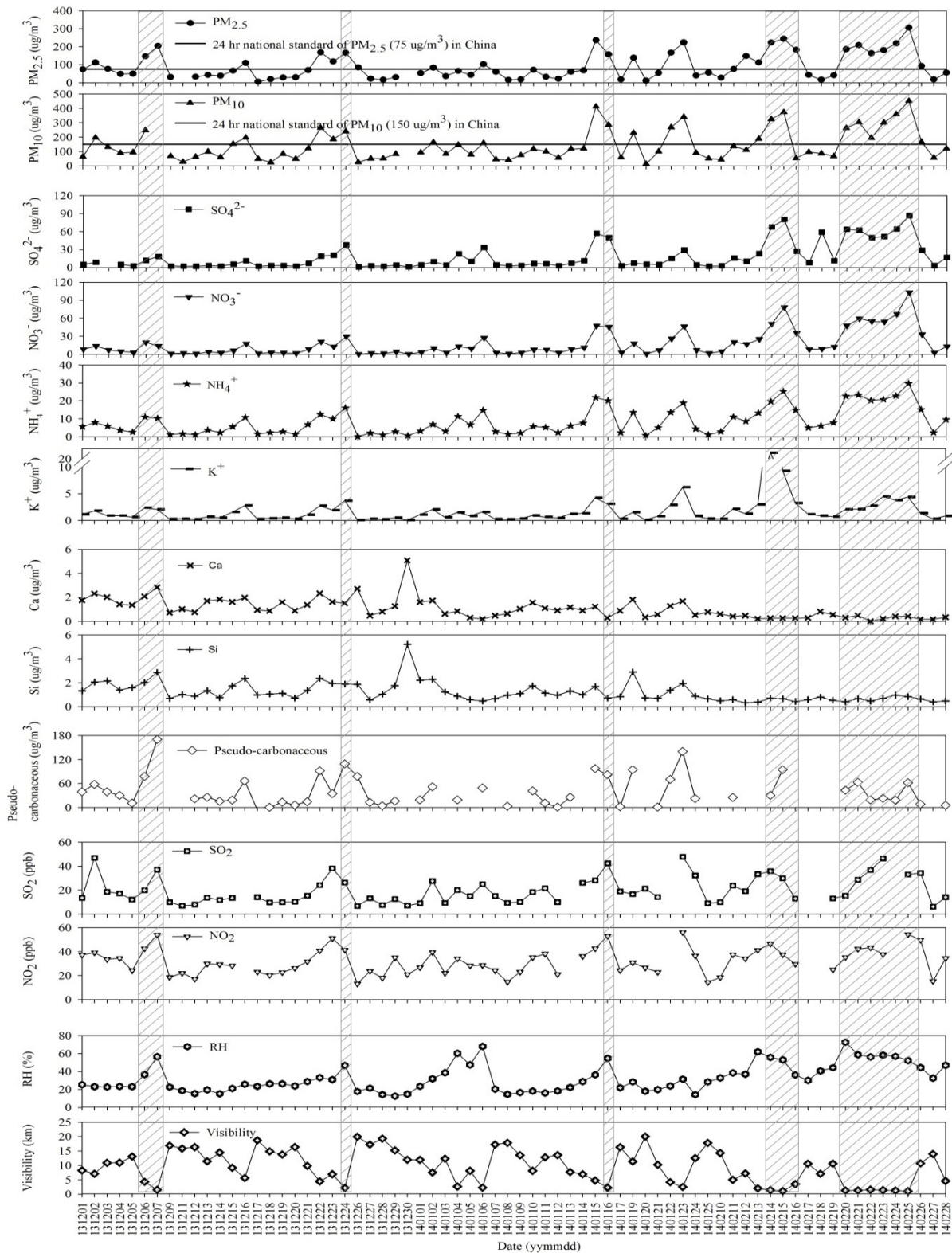
Figure 1. Variations in mass and chemical compostions of PM$_{2.5}$, PM$_{10}$ mass, gaseous precursors, and meteorological parameters measured from Dec. 1, 2013 to Feb. 28, 2014. Horizontal lines indicate the Chinese national standards of PM concentrations in 24 h and the vertically shaded regions denote the 13 haze days.

24

602
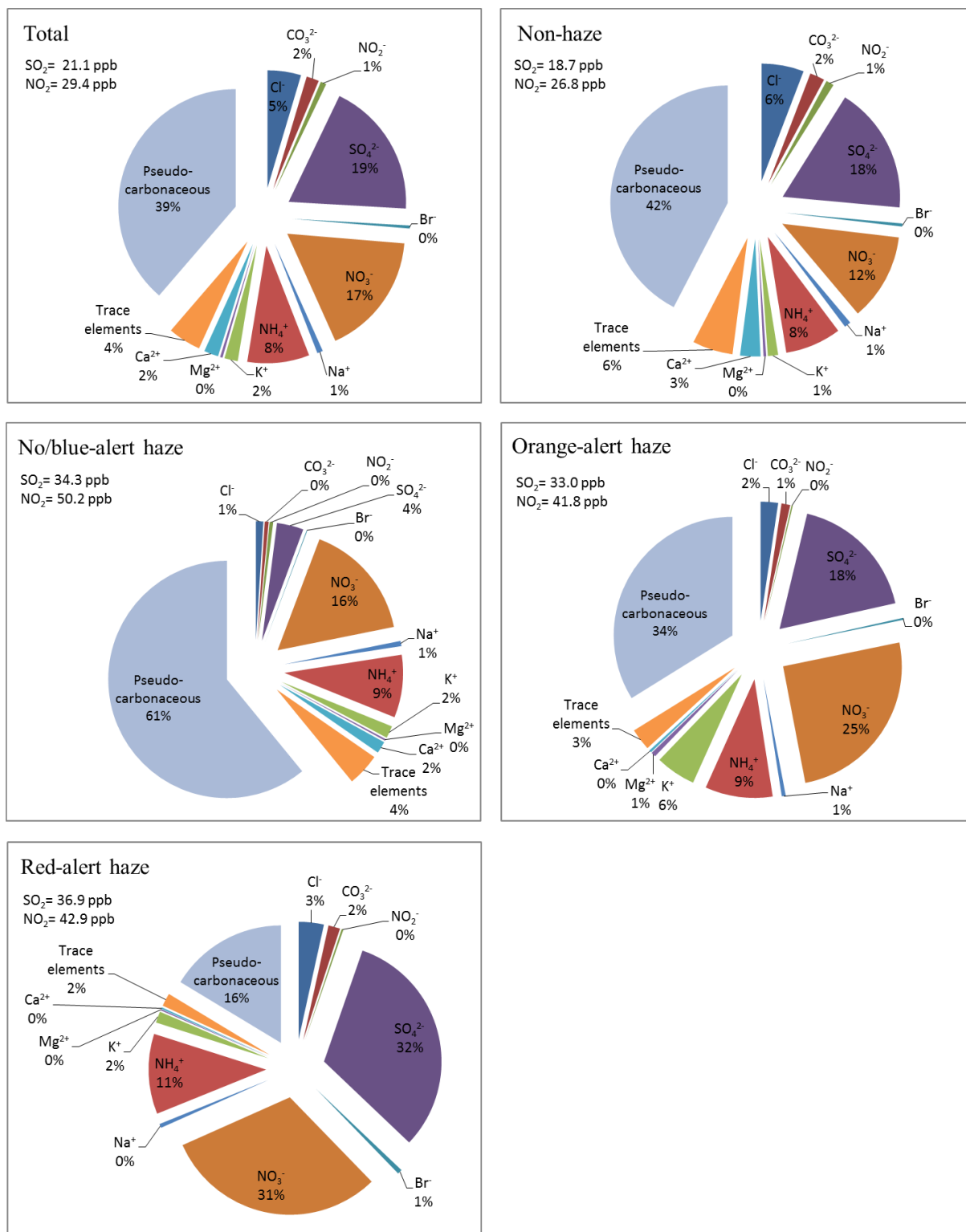
Figure 2. $PM_{2.5}$ mass contributions of water-soluble ions, trace elements, and pseudo-carbonaceous matter during the entire period (top left), non-haze days (top right), and haze days at blue-alert (center left), orange-alert (center right), and red-alert (bottom left) warning levels. The average SO_2 and NO_2 concentrations are also given.

607
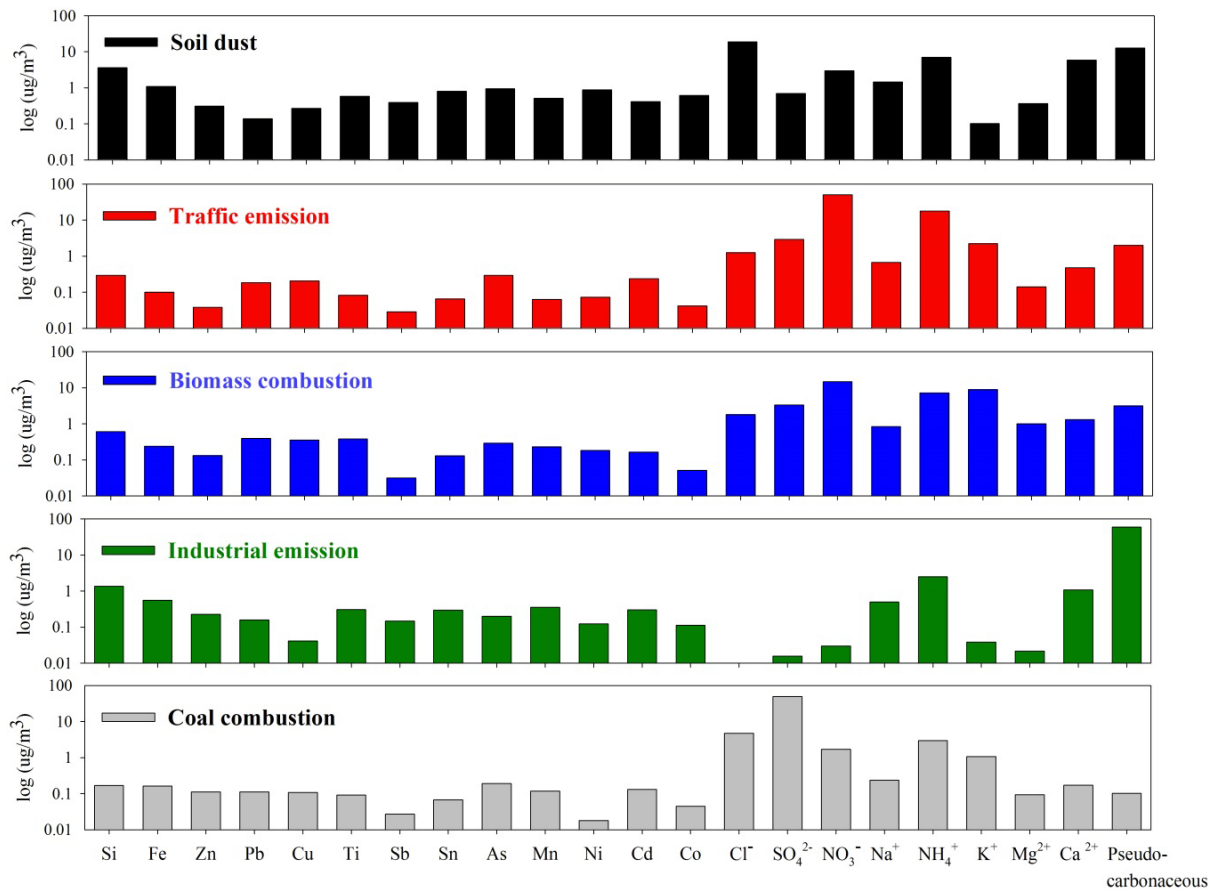
Figure 3. Composition profiles of the five factors identified in NMF analysis.
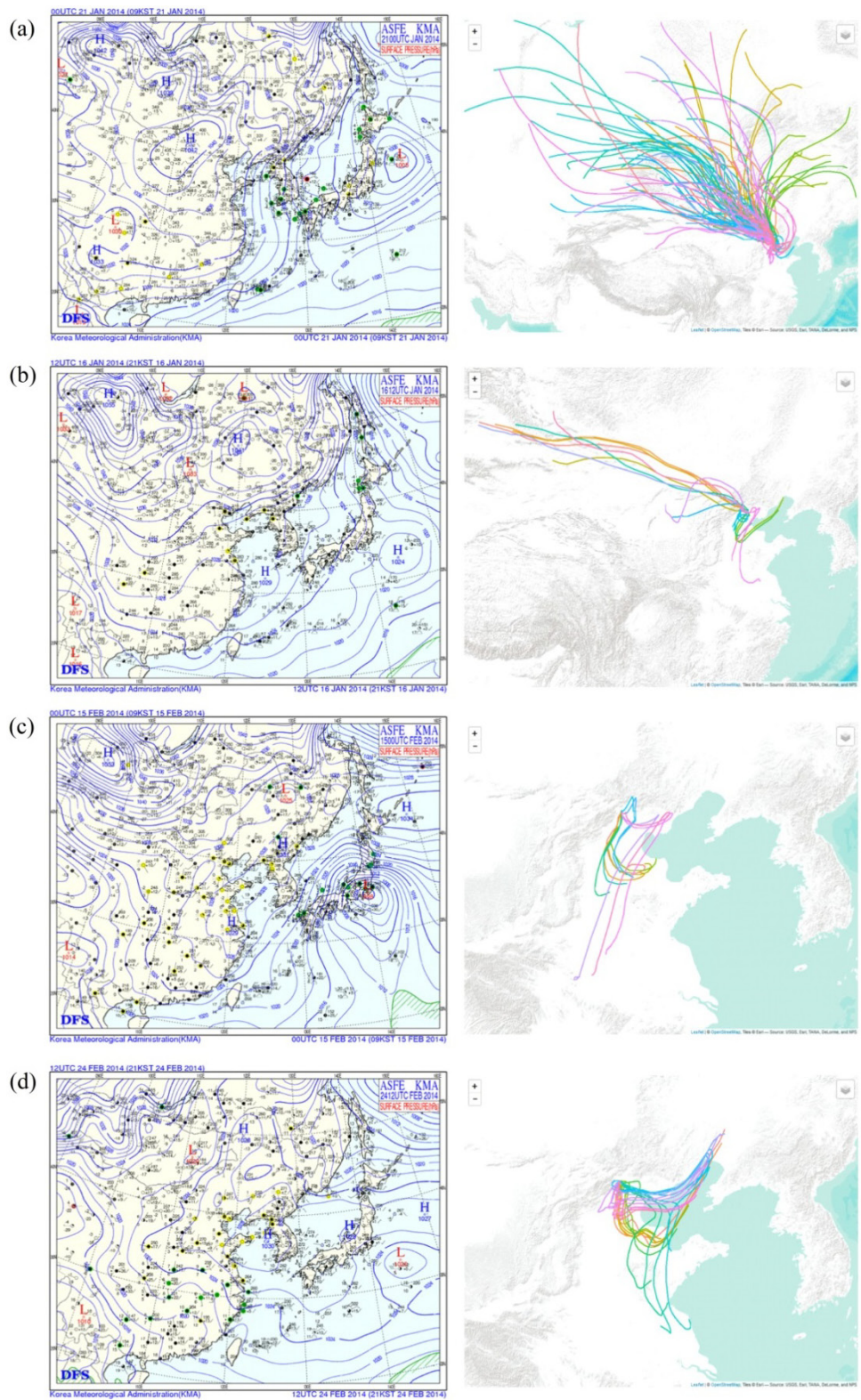
Figure 4. Surface weather maps and 72-h backward trajectories on days of (a) non-haze (57 days), (b) no/blue-alert haze (4 days), (c) orange-alert haze (3 days), and (d) red-alert haze (6 days). Trajectories were calculated twice a day at 18 and 06 UTC for non-haze days in (a) and every 6 hours at 12, 18, 24, and 06 UTC for haze days in (b), (c), and (d).
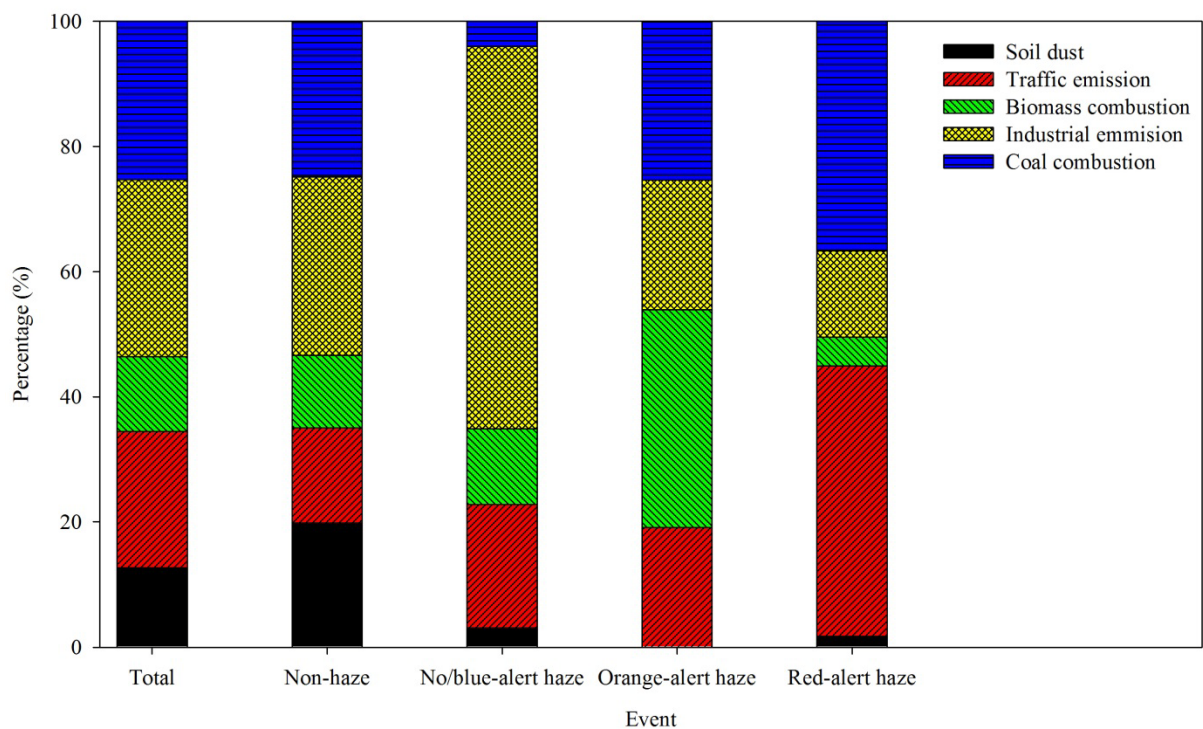
Figure 5. Comparison of source contributions (left to right) over the entire winter, during non-haze events, and during no/blue-alert, orange-alert, and red-alert haze events.